

The CD4 Determinant for Downregulation by HIV-1 Nef Directly Binds to Nef. Mapping of the Nef Binding Surface by NMR[†]

Stephan Grzesiek,^{*,‡} Stephen J. Stahl,[§] Paul T. Wingfield,[§] and Ad Bax[‡]

Laboratory of Chemical Physics, Building 5, National Institute of Diabetes and Digestive and Kidney Diseases, National Institutes of Health, Bethesda, Maryland 20892-0520, and Protein Expression Laboratory, Building 6B, National Institute of Arthritis and Musculoskeletal Diseases, National Institutes of Health, Bethesda, Maryland 20892

Received May 10, 1996; Revised Manuscript Received June 24, 1996[⊗]

ABSTRACT: Using heteronuclear NMR spectroscopy, we demonstrate that a 13-residue peptide (MSQIKRLLSEKKT) from the cytoplasmic tail of CD4 binds to Nef protein. This part of CD4 is critical for downregulation of CD4 by HIV-1 Nef [Aiken et al. (1994) *Cell* 76, 853–864]. We show that a control peptide without the central dileucine does not bind to Nef. The dependence of Nef ¹H and ¹⁵N amide chemical shifts on peptide concentration indicates that the binding is in the fast chemical exchange limit, with a dissociation constant K_d of ~ 1 mM. The peptide binding site has been mapped onto the previously determined solution structure of HIV-1 Nef [Grzesiek et al. (1996) *Nat. Struct. Biol.* 3, 340–345] on the basis of peptide-induced chemical shift changes. It comprises amino acids W57, L58, E59, G95, G96, L97, R106, and L110. When Nef is complexed to the SH3 domain of Hck tyrosine protein kinase, the peptide binds to the same site on Nef but with slightly higher affinity ($K_d \sim 0.5$ mM). This indicates that the binding of CD4 and Hck SH3 to Nef are two compatible and slightly cooperative events.

HIV-1¹ Nef is a 206-residue, N-terminal myristylated and membrane-associated protein that is expressed at high levels in the early stages of HIV infection (Cullen, 1994). Today, it is the only member of a group of so-called accessory proteins in primate lentiviruses for which the three-dimensional structure has been solved (Grzesiek et al., 1996). Although early reports suggested a negative effect on viral replication (Luciw et al., 1987; Ahmad & Venkatesan, 1988; Cheng-Mayer et al., 1989; Niederman et al., 1989), more recent evidence has established a positive role of *nef* in viral replication and disease pathogenesis (Kestler et al., 1991; Daniel et al., 1992; Zazopoulos et al., 1992; de Ronde et al., 1992; Miller et al., 1994; Spina et al., 1994; Deacon et al., 1995; Kirchhoff et al., 1995; Whatmore et al., 1995).

Infection by HIV-1 results in a significant downregulation of CD4, a type I integral membrane protein which is essential for T-cell activation and also serves as a specific receptor for the HIV-1 virus [for a recent review, see Bour et al. (1995)]. This downregulation occurs in part in the endoplasmic reticulum and results from trapping or degradation of CD4 by HIV-1 envelope glycoprotein 160 (Crise et al., 1990; Jabbar & Nayak, 1990) or the Vpu protein (Willey et al., 1992), respectively. In addition, both HIV-1 and SIV Nef downregulate cell-surface CD4, even in the absence of other viral gene products (Benson et al., 1993; Garcia et al., 1993; Foster et al., 1994; Garcia & Miller 1991; Guy et al., 1987;

Skowronski et al., 1993). CD4 downregulation and enhancement of viral infectivity by Nef seem to be dissociated events (Goldsmith et al., 1994; Chowers et al., 1995; Saksela et al., 1995). In Nef, a highly conserved proline-x-x repeat (amino acids 69–78), reminiscent of SH3 binding motifs (Shugars et al., 1993; Saksela et al., 1995), is critical for the viral infectivity enhancement function but is not essential for CD4 downregulation (Goldsmith et al., 1994; Saksela et al., 1995). On the other hand, the membrane-targeting sequence at the Nef N-terminus and a glutamic acid rich region (amino acids 60–71) preceding the Pxx repeat are important for both functions (Goldsmith et al., 1994; Aiken et al., 1994).

Downregulation of CD4 by Nef occurs by posttranslational endocytosis after CD4 has been transported to the plasma membrane in a tight complex with the T-cell tyrosine kinase p56^{lck} (Aiken et al., 1994; Rhee & Marsh, 1994). In Nef-expressing cell lines an accelerated dissociation of this CD4–p56^{lck} complex is observed (Rhee & Marsh, 1994), but conflicting evidence exists for a negative (Goldsmith et al., 1994) or positive (Bandres et al., 1995) effect of p56^{lck} on the downregulation of CD4 by Nef. The C-terminal cytoplasmic tail of CD4 is required for this downregulation by Nef (Garcia et al., 1993). This CD4 C-terminal region is also sufficient for the downregulation, since CD8 molecules which are normally unaffected by Nef become downregulated when the CD8 cytoplasmic domain is replaced by the CD4 cytoplasmic domain (Aiken et al., 1994; Anderson et al., 1994). Within this cytoplasmic tail (amino acids 396–433 of CD4), the last 15 amino acids can be deleted without affecting the downregulation (Aiken et al., 1994; Anderson et al., 1994). In contrast, the requirement of amino acids 408–418 of CD4 and in particular of the dileucine L413/L414 for the downregulation by Nef has been established by site-directed mutagenesis (Aiken et al., 1994; Anderson et al., 1994; Salghetti et al., 1995). This Nef

[†] This work was supported by the AIDS Targeted Anti-Viral Program of the Office of the Director of the National Institutes of Health.

* Corresponding author.

[‡] Laboratory of Chemical Physics, NIDDK.

[§] Protein Expression Laboratory, NIAMS.

[⊗] Abstract published in *Advance ACS Abstracts*, July 15, 1996.

¹ Abbreviations: CD4, cluster determinant 4; DTT, dithiothreitol; FID, free induction decay; HIV-1, human immunodeficiency virus type 1; HSQC, heteronuclear single-quantum correlation; NOE, nuclear Overhauser enhancement; P_{AA}, 13-residue peptide MSQIKRAASEKKT; P_{LL}, 13-residue peptide MSQIKRLLSEKKT; SH3, Src homology domain 3; SIV, simian immunodeficiency virus.

susceptibility motif in the cytoplasmic domain of CD4 overlaps at least in part with amino acids involved in the binding of CD4 to p56^{lck}, but two cysteines (420 and 422) important for the p56^{lck} association are dispensable for the Nef-induced downregulation (Aiken et al., 1994; Anderson et al., 1994; Salghetti et al., 1995).

Although direct interaction of Nef with either CD4 or p56^{lck} or their complex seems an appealing model which would unify many of the experimental observations, experimental evidence for such an association has been contradictory: Direct interaction between Nef and CD4 has been reported in baculovirus-infected Sf9 cells (Harris & Neil, 1994) and in the yeast two-hybrid system (Rossi et al., 1996). However, attempts to coimmunoprecipitate Nef and CD4 in other cellular systems have failed (Aiken et al., 1994; Anderson et al., 1994). Likewise, binding of Nef ($K_d \sim 250$ nM) — and also of a Nef peptide containing the polyproline repeat — to the Hck SH3 domain has been reported as one of the strongest SH3-mediated interactions, but no binding of this Nef peptide to p56^{lck} SH3 was found in a filter binding assay (Saksela et al., 1995; Lee et al., 1995). Recently, however, direct interaction of Nef and p56^{lck} has been shown by coimmunoprecipitation (Greenway et al., 1995; Collette et al., 1996).

In this report we show by solution NMR spectroscopy that a 13 amino acid peptide (MSQIKRLLSEKKT), i.e., amino acids 407–419 of the cytoplasmic tail of CD4, binds directly to Nef mutants lacking the N-terminal membrane targeting signal. The chemical shift changes of the Nef amide ¹H and ¹⁵N nuclei induced by peptide binding are mapped onto the solution structure of Nef (Grzesiek et al., 1996). They delineate a binding surface encompassing amino acids W57, G96, R106, and I109. The peptide binding is in the fast chemical exchange limit and relatively weak ($K_d \sim 1$ mM). However, when the same binding experiments are carried out for the peptide and the strongly bound Nef–Hck SH3 complex, the binding affinity increases ($K_d \sim 0.5$ mM), whereas the pattern of chemical shift changes remains largely unchanged.

MATERIALS AND METHODS

Sample Preparation. The following uniformly ¹⁵N-labeled Nef (strain BH10) protein constructs, all containing a Cys206 → Ala mutation, were prepared as described in Grzesiek et al. (1996): a deletion of residues 2–39 (Nef^{Δ2–39}), a deletion of residues 2–39 and of a part of a long solvent-exposed loop (Grzesiek et al., 1996) comprising residues 159–173 (Nef^{Δ2–39,Δ159–173}), and a Thr71 → Arg mutant of the latter construct (Nef^{Δ2–39,Δ159–173,T71R}). The sequence numbering for Nef is the same as given by Shugars et al. (1993). The non-isotope-labeled SH3 domain of murine Hck tyrosine protein kinase was generated as described before (Grzesiek et al., 1996). The two peptides MSQIKRLLSEKKT (P_{LL}) and MSQIKRAASEKKT (P_{AA}) were prepared using an Applied Biosystems 430A peptide synthesizer and purified by reverse-phase HPLC. For each of the titration experiments, 400 μL solutions of 0.6 mM Nef (uniformly labeled in ¹⁵N), 5 mM Tris (nondeuterated), and 10 mM DTT (nondeuterated), pH 8.1 (95% H₂O/5% D₂O), were prepared in a 5 mm NMR sample tube. For the titration of the Nef–SH3 complex the solutions contained additionally 0.6 mM Hck SH3. In order to keep dilution and NMR signal loss at

a minimum, titrations with the two peptides were carried out by adding microliter amounts of concentrated peptide stock solutions of either 7.5 or 30 mM to the NMR samples. Concentrations of the peptide stock solutions were derived from the dry weight of the lyophilized peptide. The accuracy of the concentrations of P_{AA} relative to P_{LL} and Nef was verified by quantitative, one-dimensional ¹H NMR spectroscopy. Corresponding aliquots of the peptide solution were applied through a disposable glass micropipet to the sample inside the NMR tube at room temperature followed by thorough stirring. Thereafter, for each titration point a one-dimensional proton spectrum (1–1 echo; Sklenar & Bax, 1987) and a two-dimensional water flip-back ¹⁵N-edited HSQC spectrum (Grzesiek & Bax, 1993) were recorded at 308 K.

NMR Spectroscopy. All NMR experiments were carried out on a Bruker AMX-600 spectrometer, equipped with a triple-resonance probe head that contained a self-shielded z-gradient coil. The ¹⁵N-edited HSQC data were recorded as 512 (100) complex points, with 55 ms (60 ms) acquisition times, apodized by 60° shifted sine-squared (sine) window functions, and zero filled to 1024 (512) points for ¹H (¹⁵N), respectively. A total of 12 scans per FID was accumulated, leading to a measuring time of 40 min per HSQC spectrum.

RESULTS AND DISCUSSION

CD4 Peptide Titration: Nef Amide Chemical Shifts. Quantification of chemical shift changes in a protein upon ligand binding is a sensitive method for measuring the strength of such interactions and for defining the protein's interaction surface (Otting et al., 1990; Görlach et al., 1992; Chen et al., 1993; Emerson et al., 1995). In the present study we use two-dimensional ¹H–¹⁵N NMR spectroscopy to monitor the chemical shift changes observed in several Nef mutants upon binding of the peptide P_{LL} of the CD4 cytoplasmic tail and a control peptide, P_{AA}.

In the cellular environment, Nef is anchored to the membrane via an N-terminal myristyl group. In aqueous solution, full-length Nef aggregates at the concentrations needed for detailed NMR studies, but this aggregation is alleviated for mutants lacking the N-terminal 38 residues. Comparison of two-dimensional ¹H–¹⁵N NMR spectra recorded for truncated and full-length Nef indicates that the ca. 50 N-terminal residues are highly flexible, with near-random coil chemical shifts and very rapid exchange of the peptide amide protons with solvent. The chemical shifts for the amides in the remainder of the protein are not significantly affected by the N-terminal deletion, indicating that its structure is not influenced by this deletion (Freund et al., 1994; Bax and Wingfield, unpublished results). A further improvement in the quality of the NMR spectrum is obtained when 15 residues in a long, solvent-exposed flexible loop are deleted (Nef^{Δ2–39,Δ159–173}), again without affecting the chemical shifts or the NOE contacts for the remaining residues (Grzesiek et al., 1996). In the present study we report on the binding of the P_{LL} peptide to these two mutants and to a third mutant (Nef^{Δ2–39,Δ159–173,T71R}) where threonine 71 is replaced by an arginine. Many Nef sequences derived from HIV patients contain this mutation at residue 71, and tighter binding of Nef^{T71R} to Hck SH3 was reported (Saksela et al., 1995).

Figure 1 shows small regions of the ¹H–¹⁵N HSQC spectra of Nef for the titrations of P_{LL}–Nef^{Δ2–39} (Figure 1a–c), P_{LL}–

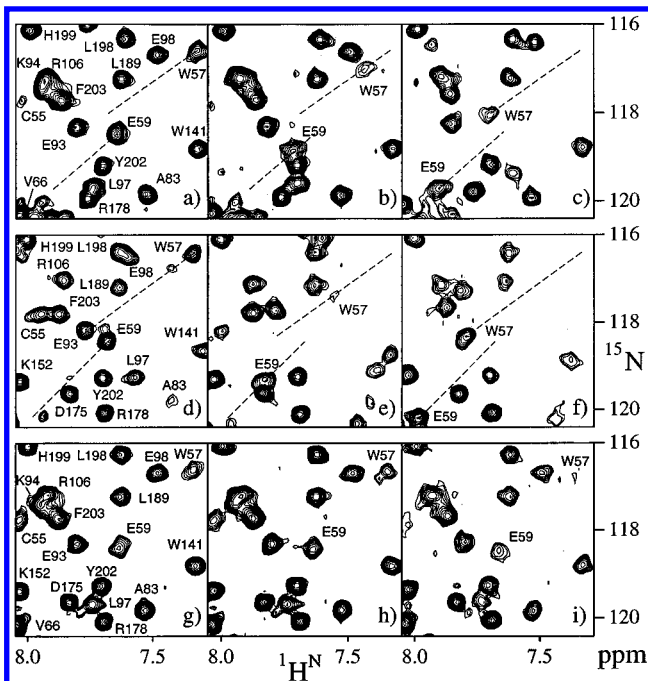


FIGURE 1: Small regions of ^1H - ^{15}N HSQC spectra of Nef as a function of added peptide P_{LL} or P_{AA} . (a–c) $\text{Nef}^{\Delta 2-39} + P_{\text{LL}}$; (d–f) $[\text{Nef}^{\Delta 2-39, \Delta 159-173, \text{T71R}} + \text{SH3}] + P_{\text{LL}}$; (g–i) $\text{Nef}^{\Delta 2-39, \Delta 159-173, \text{T71R}} + P_{\text{AA}}$. Concentrations (in mM) of Nef (peptide) are respectively (a) 0.59 (0.00), (b) 0.54 (0.61), (c) 0.49 (3.70), (d) 0.59 (0.00), (e) 0.54 (0.68), (f) 0.47 (4.10), (g) 0.65 (0.00), (h) 0.62 (0.42), and (i) 0.56 (3.62). For the $\text{Nef}^{\Delta 2-39, \Delta 159-173, \text{T71R}} + \text{SH3}$ complex the SH3 concentration equals the Nef concentration.

$\text{Nef}^{\Delta 2-39, \Delta 159-173, \text{T71R}} + \text{SH3}$ (Figure 1d–f), and the control $P_{\text{AA}} - \text{Nef}^{\Delta 2-39, \Delta 159-173, \text{T71R}}$ (Figure 1g–i). Columns 1–3 in Figure 1 correspond to molar ratios of peptide to Nef of approximately 0, 1, and 7, respectively. Besides an overall line broadening with increasing addition of peptide ($\sim 25\%$ for the highest peptide concentration) the spectra remain largely the same, and chemical shift changes occur only for a small number of residues in the case of P_{LL} (Figure 1a–c, d–f). The observed chemical shift changes are a continuous and monotonic function of the amount of added peptide, which indicates that binding of P_{LL} to Nef or Nef + SH3 is in the fast chemical exchange limit on the NMR time scale. No chemical shift changes are observed when the control peptide, P_{AA} , is added (Figure 1g–i).

The largest amide chemical shift changes are observed for residues close to W57 in the primary sequence, and the path of the W57 and E59 resonances during the titration has been marked in Figure 1. Interestingly, all three Nef mutants have the same binding affinity to P_{LL} (see below, Figure 2), and their chemical shifts change in the same way during the titration with P_{LL} (data not shown). This indicates that the conformationally disordered loop connecting β strands 4 and 5 (residues 146–181) is not involved in the interaction with the CD4 peptide. Neither is this loop involved in the binding of Nef to Hck SH3 (Grzesiek et al., 1996). Similarly, the binding behavior of P_{LL} to Nef or the Nef–SH3 complex is not affected by the point mutation T71R; i.e., for both $\text{Nef}^{\Delta 2-39, \Delta 159-173}$ and $\text{Nef}^{\Delta 2-39, \Delta 159-173, \text{T71R}}$ the same binding affinity and pattern of chemical shift changes is observed (data not shown).

Figure 1d–f shows the titration of the complex of $\text{Nef}^{\Delta 2-39, \Delta 159-173, \text{T71R}}$ and Hck SH3 with the P_{LL} peptide. Upon addition of P_{LL} , significant amide chemical shift changes are

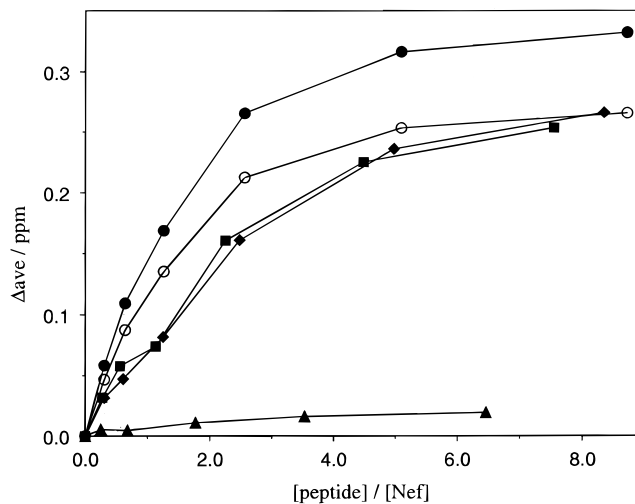


FIGURE 2: Weighted average of the E59 amide ^1H and ^{15}N chemical shift changes, Δ_{av} ($\Delta_{\text{av}} = [(\Delta\delta_{\text{HN}}^2 + \Delta\delta_{\text{N}}^2/25)]^{1/2}$), as a function of the molar ratio of peptide to Nef. Symbols: (■) $\text{Nef}^{\Delta 2-39} + P_{\text{LL}}$; (◆) $\text{Nef}^{\Delta 2-39, \Delta 159-173, \text{T71R}} + P_{\text{LL}}$; (●) $[\text{Nef}^{\Delta 2-39, \Delta 159-173, \text{T71R}} + \text{SH3}] + P_{\text{LL}}$; (○) same as (●) but scaled vertically by 0.8; (▲): $\text{Nef}^{\Delta 2-39, \Delta 159-173, \text{T71R}} + P_{\text{AA}}$. Nef concentrations during the titration were ~ 0.5 – 0.6 mM (see Figure 1).

observed for the same amino acids as for free Nef, with the largest changes again around W57. However, some of the changes are more pronounced: For example, the amide proton of W57 shifts by 0.3 ppm for free Nef (Figure 1a–c) and by 0.4 ppm for the Nef–SH3 complex (Figure 1d–f), whereas the amide nitrogen of E93 shifts by 0.3 and 1 ppm in the free and complexed form, respectively.

As a control for the specificity of binding, a titration of Nef was carried out with the P_{AA} peptide where the critical dileucine motif of P_{LL} is replaced by two alanines. Results shown in Figure 1g–i indicate the absence of any significant Nef amide chemical shift changes, including those residues which are affected most by the binding of P_{LL} (e.g., W57, L58, E59, or L117). However, at the highest peptide concentration (3.6 mM) some line broadening occurs which is not limited to residues in the P_{LL} binding region. Apparently, this is a result of a much weaker and nonspecific interaction.

Binding Affinity of P_{LL} and Nef. Figure 2 shows the weighted average of the E59 amide ^1H and ^{15}N chemical shift changes, Δ_{av} , as a function of the molar ratio of peptide to Nef. Clearly, complex formation of P_{LL} with $\text{Nef}^{\Delta 2-39}$ (■) or with the loop deletion mutant $\text{Nef}^{\Delta 2-39, \Delta 159-173, \text{T71R}}$ (◆) is indistinguishable. The chemical shift changes of the amide of E59 are, however, slightly larger when $\text{Nef}^{\Delta 2-39, \Delta 159-173, \text{T71R}}$ is complexed to the Hck SH3 domain (●). Under saturating conditions Δ_{av} reaches a value of >0.33 ppm for the Nef–SH3 complex whereas for Nef without SH3 Δ_{av} levels off at about 0.28 ppm. Larger amide chemical shift changes in Nef–SH3 are also observed for other amino acids, e.g., W57 (see above), and a similar increase in chemical shift changes is found for the ^1H methyl resonances of L97 which are resolved in the upfield region of the proton spectrum (Figure 3). The L97 $\delta 1$ and L97 $\delta 2$ ^1H resonances shift by 0.03 and 0.05 ppm, respectively, when $\text{Nef}^{\Delta 2-39, \Delta 159-173, \text{T71R}}$ is saturated by P_{LL} (Figure 3A) but shift by 0.06 and 0.09 ppm for the $\text{Nef}^{\Delta 2-39, \Delta 159-173, \text{T71R}}$ –Hck SH3 complex (Figure 3B).

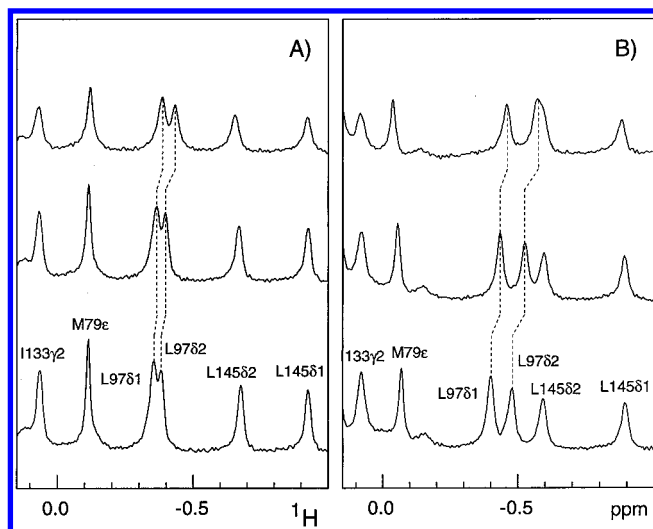


FIGURE 3: Chemical shift changes in the resolved methyl region of the ^1H spectrum of Nef in the presence of increasing amounts (from bottom to top) of peptide P_{LL} . Panels: (A) $\text{Nef}^{\Delta 2-39, \Delta 159-173, \text{T71R}}$; (B) $\text{Nef}^{\Delta 2-39, \Delta 159-173, \text{T71R}} + \text{Hck SH3}$ (1:1 complex). Nef and peptide concentrations (in mM) were respectively (A) 0.56, 0 (bottom), 0.51, 0.64 (middle), and 0.46, 8.35 (top) and (B) 0.59, 0.0 (bottom), and 0.54, 0.68 (middle), and 0.47, 8.72 (top).

For E59, the difference in amide proton chemical shifts between free Nef and peptide-saturated Nef is 0.3 ppm (=180 Hz) for both $\text{Nef}^{\Delta 2-39}$ (Figure 1a–c) and $\text{Nef}^{\Delta 2-39, \Delta 159-173, \text{T71R}} + \text{SH3}$ (Figure 1d–f). As the resonance for E59 is broadened by only ~ 13 Hz for nonsaturating concentrations of the peptide P_{LL} (Figure 1b,e), the exchange between the bound and free state is considerably faster than 180 Hz.

For the $\text{Nef}^{\Delta 2-39, \Delta 159-173, \text{T71R}}-\text{SH3}$ complex, the midpoint of the chemical shift changes is observed at a molar ratio of P_{LL} to Nef of ~ 1.3 (Figure 2). This ratio is significantly lower than the midpoint ratio of > 2.2 , found for the titration of either $\text{Nef}^{\Delta 2-39}$ or $\text{Nef}^{\Delta 2-39, \Delta 159-173, \text{T71R}}$ (Figure 2). These results indicate that P_{LL} binds to Nef–SH3 with a higher affinity than to Nef alone. Assuming a simple binary reaction between Nef and P_{LL} , analysis by nonlinear curve fitting yields values for K_d of 0.49 ± 0.09 , 1.18 ± 0.21 , and 1.43 ± 0.26 mM for $\text{Nef}^{\Delta 2-39, \Delta 159-173, \text{T71R}} + \text{SH3}$, $\text{Nef}^{\Delta 2-39}$, and $\text{Nef}^{\Delta 2-39, \Delta 159-173, \text{T71R}}$, respectively. Errors in this fit take into account the accuracy of the fit and the reproducibility of fitting the chemical shift changes for two different residues (E59 and W57) for the same titration, as well as the reproducibility of two independent titrations. To illustrate more clearly this difference in affinity for Nef–SH3 and Nef alone, open circles in Figure 2 show the titration results for $\text{Nef}^{\Delta 2-39, \Delta 159-173, \text{T71R}}-\text{SH3}$ with the last point scaled to the last point of the $\text{Nef}^{\Delta 2-39, \Delta 159-173, \text{T71R}}$ titration. As already evidenced in Figure 1g–i, titration of $\text{Nef}^{\Delta 2-39, \Delta 159-173, \text{T71R}}$ with the control peptide P_{AA} does not result in significant changes of the E59 amide shifts (Figure 2, \blacktriangle).

Mapping of the Nef CD4 Binding Surface. The amide chemical shift changes in $\text{Nef}^{\Delta 2-39}$ induced by binding P_{LL} are shown as a function of residue number in Figure 4A. The largest changes are clustered around residues L58, G96, and L110, sites which are clearly different from the locations of maximal chemical shift change observed upon complex formation between $\text{Nef}^{\Delta 2-39, \Delta 159-173}$ and Hck SH3 (Grzesiek et al., 1996). The latter changes (Figure 4B) are observed mainly in the region of the Pxx repeat (residues Q73 and V74) and near residue H116. Most of the Nef side chain

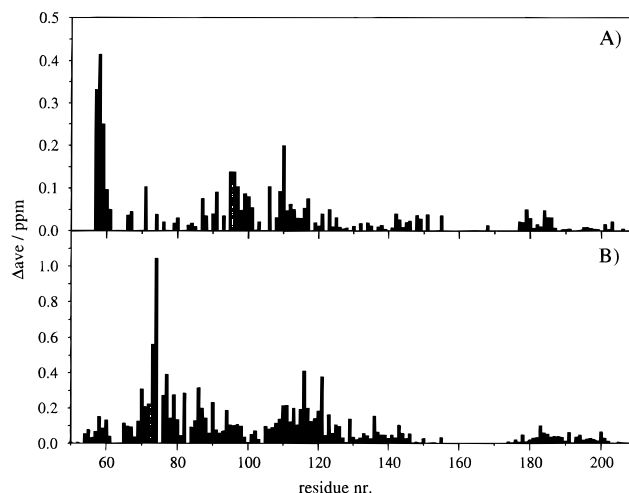
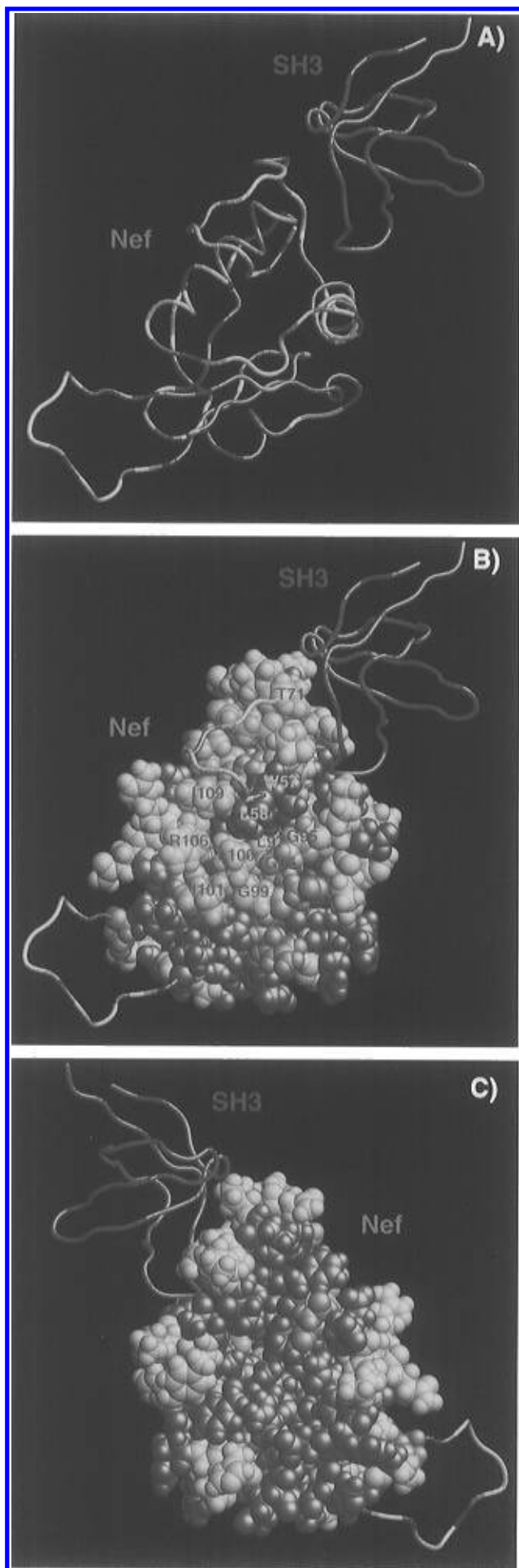


FIGURE 4: (A) Average amide chemical shift changes Δ_{av} in Nef induced upon binding of P_{LL} to $\text{Nef}^{\Delta 2-39}$ as a function of residue number (0.49 mM $\text{Nef}^{\Delta 2-39}$, 3.70 mM P_{LL}). (B) Average chemical shift changes of the $^1\text{H}_\text{N}$, ^{15}N , $^{13}\text{C}_\alpha$, $^{13}\text{C}_\beta$ nuclei observed in $\text{Nef}^{\Delta 2-39, \Delta 159-173}$ (Grzesiek et al., 1996) induced upon binding of SH3 (1:1 complex). The average change in chemical shift was calculated as $[(\Delta\delta^2_{\text{HN}} + \Delta\delta^2_{\text{N}}/25 + \Delta\delta^2_{\text{C}\alpha}/4 + \Delta\delta^2_{\text{C}\beta}/4)/4]^{1/2}$.

Gln and Asn $^{15}\text{N}-^1\text{H}_2$ resonances have not been assigned sequence specifically. Upon binding of P_{LL} to Nef, however, only one $^{15}\text{N}-^1\text{H}_2$ resonance pair, presumably belonging to Q61, shifts measurably (maximal $\Delta_{\text{av}} = 0.14$). Two (W57 and W113) of the five Trp side chain NeH groups also show considerable perturbations (maximal $\Delta_{\text{av}} = 0.26$ and 0.11, respectively). This coincides with the significant perturbation of the backbone amide resonances observed for these residues (Figure 4A).

The amide chemical shift changes induced by P_{LL} binding are color coded on a tubular representation of the backbone of $\text{Nef}^{\Delta 2-39, \Delta 159-173}$ (Figure 5A) as well as on a space-filling model (Figure 5B,C). The residues most strongly affected by binding (W57, L58, E59, A60, G95, G96, L97, R106, I109, L110) delineate a hydrophobic patch on the surface of Nef which is centered at the HIV protease cleavage site (residues W57, L58; Freund et al., 1994). This interaction surface comprises the protease cleavage site itself and the first part of an extended stretch connecting helices 1 and 2, i.e., G95, G96, and L97, as well as the inner side of the N-terminal part of helix 2. The chemical shift changes seen for the H^N and N resonances of T71 ($\Delta_{\text{av}} \sim 0.1$ ppm, color coded in yellow in Figure 5), which is separated from the other residues affected by P_{LL} binding, presumably reflect a slight rearrangement of the C-terminal end of helix 2 which is in contact with T71. The same chemical shift changes are seen for the H^N and N resonances of R71 in the T71R Nef constructs.

Residues W57, L58, and E59 at the HIV protease cleavage site are the most strongly affected by the binding of the peptide P_{LL} . These amino acids are followed in the primary sequence by residues A60 to F68 which connect the HIV protease cleavage site to the polyproline repeat. On the basis of ^{15}N relaxation measurements (S. Grzesiek, N. Tjandra, S. Stahl, P. Wingfield, and A. Bax, manuscript in preparation) residues 59–70 are highly mobile and their structure is not very well defined (Grzesiek et al., 1996). Residues 55–59 are considerably less mobile, while the observation of amide protons for residues N-terminal of C55 is severely hindered by the fast exchange with bulk water.



However, the contact between the protease cleavage site and the extended stretch between helices 1 and 2 and also the first part of helix 2 is well established by a set of unambiguous NOEs from amino acids W57 and L58 to G95, L97, L100, I109, and L110. Interestingly, the mobile region between E59 and V70 contains a highly conserved cluster of negatively charged residues, i.e., E62, E63, E64, E65 (Shugars et al., 1993), that could interact favorably with positive charges on the CD4 molecule which harbors 8 arginines and 4 lysines in the 40 residues of its cytoplasmic tail (Bour et al., 1995).

The highly conserved Nef residues V74 and R77, corresponding to the canonical P_0 and P_{-3} binding positions for SH3 domains, indicate binding of Nef to Hck SH3 in the minus orientation (Lim et al., 1994; Feng et al., 1994). Together with the known structure of a polyproline/SEM5–SH3 complex (Lim et al., 1994) and the chemical shift changes on the Nef surface induced by SH3 binding, this provided enough information for modeling the position of the bound SH3 domain (Grzesiek et al., 1996). Figure 5 also shows this modeled position of the SH3 domain (SEM5, magenta). Our results indicate that the position of the SH3 domain does not obstruct Nef's interaction surface with the CD4 peptide. As the RT loop of the SH3 domain inserts itself between helices 1 and 2, we hypothesize that binding of the SH3 domain to Nef slightly widens the space between residues 57/58 and its surrounding neighbors (Figure 5B). This could expose a larger hydrophobic interaction area, namely, a larger surface of leucine and isoleucine residues (e.g., L58, L97, L100, I109), to the P_{LL} dileucine motif, thereby enhancing its binding affinity to Nef. The more pronounced chemical shift changes for the amide nuclei (Figures 1 and 2) and methyl resonances of L97 (Figure 3) observed upon binding of P_{LL} to the Nef–SH3 complex as compared to Nef alone corroborate this hypothesis.

CONCLUSION

In this report we have demonstrated that Nef, without any accessory proteins, is able to bind to a peptide (MS-QIKRLLSEKKT) of the CD4 cytoplasmic tail which is essential for the CD4 downregulation function of Nef (Aiken et al., 1994; Anderson et al., 1994; Salghetti et al., 1995). Although the affinity is relatively low ($K_d \sim 1$ mM), this binding is nevertheless specific as it delineates a well-defined

FIGURE 5: Backbone worm (A) and space-filling (B, C) models of Nef with color coding to show those residues whose amide H_N and ^{15}N resonances are most affected upon binding the CD4 peptide P_{LL} . Coordinates correspond to the solution structure of Nef $^{\Delta 2-39, \Delta 159-173}$ (Grzesiek et al., 1996) further refined by additional long-range NOEs. Unstructured residues N-terminal of A56 are not shown. Amino acids 59–70 and 149–178 which are highly flexible in the NMR structure are represented as a backbone worm in (B) and (C). The putative position of an SH3 domain (magenta) in complex with Nef is shown as modeled previously (Grzesiek et al., 1996). The mean chemical shift difference Δ_{av} (Figure 3A) for each amino acid is displayed in colors ranging from dark blue ($\Delta_{av} < 0.05$ ppm) to blue ($\Delta_{av} < 0.07$ ppm), light blue ($\Delta_{av} < 0.08$ ppm), light green ($\Delta_{av} < 0.1$ ppm), yellow ($\Delta_{av} < 0.13$ ppm), brown ($\Delta_{av} < 0.16$ ppm), and red ($\Delta_{av} \geq 0.16$ ppm). For some residues (color coded in gray) the chemical shift changes could not be identified because of overlap in the random coil region of the 1H – ^{15}N HSQC spectrum or because of fast exchange of the amide protons with solvent (residues 1, 39–56, 157, 158, 176, 193). Representations A and B are drawn in the same orientation whereas representation C is rotated by 180° around the vertical axis.

area on the surface of Nef and is abrogated when the critical central dileucine motif is replaced by two alanines. Furthermore, this binding affinity increases 2-fold when Nef is complexed to the SH3 domain of Hck. The relatively low affinity of the peptide does not necessarily translate into a low concentration of the Nef-CD4 complex in the physicochemical environment of a T-cell. First, the complete C-terminal domain of CD4 might exhibit a higher affinity in its folded form at the membrane surface. Second, an additional, yet unidentified protein could enhance the affinity further in a ternary or quaternary complex. Third, the CD4 C-terminus and Nef are both anchored to the cellular membrane and therefore restricted to a small interaction volume within the T-cell. Local concentrations of both CD4 and Nef are therefore considerably higher than in the case where these proteins are uniformly distributed throughout the cell. For example, if we assume an interaction volume of 5 nm thickness at the membrane and a spherical T-cell with a radius on the order of 5–10 μm , for a given number of molecules, the local concentrations at the membrane would increase by 2 orders of magnitude over concentrations resulting from a uniform distribution within the whole internal T-cell volume. At this moment, there is conflicting evidence about the presence of Nef-CD4 complexes in vivo (Harris & Neil, 1994; Rossi et al., 1996; Anderson et al., 1994; Aiken et al., 1994). However, the apparent requirement of membrane anchoring of Nef for the detection of the Nef-CD4 complexes (Harris & Neil 1994) together with the low affinity and possibly transient nature of this association may have been responsible for the failure to detect such complexes by immunoprecipitation assays.

ACKNOWLEDGMENT

We thank Jon Marsh, Stephan Bour, and Andy Wang for many helpful comments on the manuscript, Marius Clore for help with the structure calculations, Nico Tjandra for analysis of the relaxation data, Ira Palmer for protein purification, Pat Spinella for peptide synthesis, and Rolf Tschudin for technical support, as well as Frank Delaglio and Dan Garrett for software support.

REFERENCES

- Ahmad, N., & Venkatesan, S. (1988) *Science* 241, 1481–1485.
- Aiken, C., Konner, J., Kandau, N. R., Lenburg, M. E., & Trono, D. (1994) *Cell* 76, 853–864.
- Anderson, S. J., Lenburg, M., Landau, N. R., & Garcia, J. V. (1994) *J. Virol.* 68, 3092–3101.
- Bandres, J. C., Shaw, A. S., & Ratner, L. (1995) *Virology* 207, 338–341.
- Benson, R. E., Sanfridson, A., Ottinger, J. S., Doyle, C., & Cullen, B. R. (1993) *J. Exp. Med.* 177, 1561–1566.
- Bour, S., Geleziunas, R., & Wainberg, M. A. (1995) *Microbiol. Rev.* 59, 63–93.
- Chen, Y., Reizer, J., Saier, M. H., & Fairbrother, W. F. (1993) *Biochemistry* 32, 32–37.
- Cheng-Mayer, C., Iannello, P., Shaw, P. A., Luciw, P. A., & Levy, J. A. (1989) *Science* 246, 1629–1632.
- Chowers, M. Y., Pandori, M. W., Spina, C. A., Richman, D. D., and Guatelli, J. C. (1995) *Virology* 212, 451–457.
- Crise, B., Buonocore, L., & Rose, J. K. (1990) *J. Virol.* 64, 5585–5593.
- Jabbar, M. A., & Nayak, D. P. (1990) *J. Virol.* 64, 6297–6304.
- Cullen, B. R. (1994) *Virology* 205, 1–6.
- de Ronde, A., Klaver, B., Keulen, W., Smit, L., & Goudsmit, J. (1992) *Virology* 188, 391–395.
- Daniel, M. D., Kirchhoff, F., Czajak, S. C., Seghal, P. K., and Desrosiers, R. C. (1992) *Science* 258, 1938–1941.
- Deacon, N. J., Tsykin, A., Solomon, A., Smith, K., Ludford-Menting, M., Hooker, D. J., McPhee, D. A., Greenway, A. L., Ellett, A., Chatfield, C., Lawson, V. A., Crowe, S., Maerz, A., Sonza, S., Learmont, J., Sullivan, J. S., Cunningham, A., Dwyer, D., Dowton, D., & Mills, J. (1995) *Science* 270, 988–991.
- Emerson, S. D., Madison, V. S., Palermo, R. E., Waugh, D. S., Scheffler, J. E., Tsao, K.-L., Kiefer, S. E., Liu, S. P., & Fry, D. C. (1995) *Biochemistry* 34, 6911–6918.
- Feng, S., Chen, J. K., Yu, H., Simon, J. A., & Schreiber, S. L. (1994) *Science* 266, 1241–1247.
- Foster, J. L., Anderson S. J., Frazier, A. L., & Garcia, J. V. (1994) *Virology* 201, 373–379.
- Freund, J., Kellner, R., Konvalinka, J., Wolber, V., Krausslich, H. G., & Kalbitzer, H. R. (1994) *Eur. J. Biochem.* 223, 589–593.
- Garcia, J. V., & Miller, A. D. (1991) *Nature* 350, 508–511.
- Garcia, J. V., Alfano, J., & Miller, A. D. (1993) *J. Virol.* 67, 1511–1516.
- Goldsmith, M. A., Warmerdam, M. T., Atchison, R. E., Miller, M. D., & Greene, W. C. (1995) *J. Virol.* 69, 4112–4121.
- Greenway, A., Azad, A., & McPhee, D. (1995) *J. Virol.* 69, 1842–1850.
- Grzesiek, S., & Bax, A. (1993) *J. Am. Chem. Soc.* 115, 12593–12594.
- Grzesiek, S., Bax, A., Clore, G. M., Gronenborn, A. M., Hu, J.-S., Kaufman, J., Palmer, I., Stahl, S. J., & Wingfield, P. T. (1996) *Nat. Struct. Bio.* 3, 340–345.
- Görlach, M., Wittekind, M., Beckman, R. A., Mueller, L., & Dreyfuss, G. (1992) *EMBO J.* 11, 3289–3295.
- Guy, B., Kieny, M. P., Riviere, Y., Le Peuch, C., Dott, K., Girard, M., Montagnier, L., & Lecocq, J. (1987) *Nature* 330, 266–269.
- Harris, M. P., & Neil, J. C. (1994) *J. Mol. Biol.* 241, 136–142.
- Kestler, H. W., Ringler, D. J., Mori, K., Panicali, D. L., Sehgal, P. K., Daniel, M. D., & Desrosiers, R. C. (1991) *Cell* 65, 651–662.
- Lee, C. H., Leung, B., Lemmon, M. A., Zheng, J., Cowburn, D., Kuriyan, J., & Saksela, K. (1995) *EMBO J.* 14, 5006–5015.
- Kirchhoff, F., Greenough, T. C., Brettler, D. B., Sullivan, J. L., & Desrosiers, R. C. (1995) *N. Engl. J. Med.* 332, 228–232.
- Lim, W. A., Richards, F. M., & Fox, R. O. (1994) *Nature* 372, 375–379.
- Luciw, P. A., Cheng-Mayer, C., & Levy, J. A. (1987) *Proc. Natl. Acad. Sci. U.S.A.* 84, 1434–1438.
- Miller, M. D., Warmerdam, M. T., Gaston, I., Greene, W. C., & Feinberg (1994) *J. Exp. Med.* 179, 101–113.
- Niederman, T. M., Thielan, B. J., & Ratner, L. (1989) *Proc. Natl. Acad. Sci. U.S.A.* 86, 1128–1132.
- Otting G., Qian, Y. Q., Billeter, M., Müller, M., Affolter, M., Gehring, W. J., & Wüthrich, K. (1990) *EMBO J.* 9, 3085–3092.
- Rhee, S. S., & Marsh J. W. (1994) *J. Virol.* 68, 5156–5163.
- Rossi, F., Gallina, A., & Milanesi, G. (1996) *Virology* 217, 397–403.
- Saksela, K., Cheng, G., & Baltimore, D. (1995) *EMBO J.* 14, 484–491.
- Salghetti, S., Mariani, R., & Skowronski, J. (1995) *Proc. Natl. Acad. Sci. U.S.A.* 92, 349–353.
- Shugars, D. C., Smith, M. S., Glueck, D. H., Nantermet, P. V., Seillier-Moiseiwitsch, F., & Swanstrom, R. (1993) *J. Virol.* 67, 4639–4650.
- Sklenar, V., & Bax, A. (1987) *J. Magn. Reson.* 74, 469–479.
- Skowronski, J., Parks, D., & Mariani, R. (1993) *EMBO J.* 12, 703–713.
- Spina, C. A., Kwok, T. J., Chowers, M. Y., Guatelli, J. C., & Richman, D. D. (1994) *J. Exp. Med.* 179, 115–123.
- Whatmore, A. M., Cook, N., Hall, G. A., Sharpe, S., Rud, E. W., & Cranage, M. P. (1995) *J. Virol.* 69, 5117–5123.
- Willey, R. L., Maldarelli, F., Martin, M. A., & Strebel, K. (1992) *J. Virol.* 66, 7193–7200.
- Zazopoulos, E., & Haseltine, W. A. (1992) *Proc. Natl. Acad. Sci. U.S.A.* 89, 6634–6639.